A comparison of modes of upwelling-favorable wind variability in the Benguela and California current ecosystems

Marisol García-Reyes[a,*], Tarron Lamont[b,c], William J. Sydeman[a,d], Bryan A. Black[e], Ryan R. Rykaczewski[f], Sarah Ann Thompson[a], Steven J. Bograd[g]

[a] Farallon Institute, 101 H St. Suite Q, Petaluma, CA 94952, USA
[b] Oceans & Coasts Research Branch, Department of Environmental Affairs, Private Bag X4390, Cape Town, 8000, South Africa
[c] Marine Research Institute and Department of Oceanography, University of Cape Town, Private Bag X3, Rondebosch, 7701, South Africa
[d] Bodega Marine Laboratory, University of California, Davis, P.O. Box 247, Bodega Bay, CA 94923, USA
[e] Marine Science Institute, University of Texas, Port Aransas, TX, USA
[f] Department of Biological Sciences & Marine Science Program, University of South Carolina, Columbia, SC, USA
[g] Environmental Research Division, Southwest Fisheries Science Center, NOAA, Monterey, California, USA
[*] Corresponding author e-mail: marisolgr@faralloninstitute.org

Abstract

The California Current System (CCS) has two independent seasonal modes of upwelling variability, summer and winter, driven by different atmospheric processes. The variability of upwelling winds during winter is particularly important as strong, episodic events, driven by atmospheric teleconnections with the equatorial Pacific that are active in this season, impact ecological systems along the west coast of North America. Given the importance of upwelling seasonality to ecosystem function, we hypothesize that the Benguela Current System (BCS) shows similar independent seasonal modes of upwelling variability. To test this hypothesis, compare modes of variability between systems, and investigate potential drivers, we use an upwelling index derived from NCEP2 wind data (1979-2014) for the

northern, southern, and Agulhas Bank areas of the BCS. In the northern and southern BCS, only one mode of upwelling variability is observed: year-round in the north and during the austral spring and summer (October through April) in the south. The Agulhas Bank region shows two modes of seasonal variability. Based on this 35-year dataset, summer upwelling modes in both the CCS and BCS appear to have similar decadal-scale variability. The other modes of variability (winter mode in the CCS and the non-seasonal second mode in the BCS) are correlated with year-to-year variability in the positioning of regional oceanic high-pressure systems. The leading mode of upwelling variability in the Agulhas Bank region, in the austral summer/fall, is highly correlated with sea level pressure as well as sea surface temperature in the equatorial Pacific, in a spatial and seasonal pattern (boreal winter) resembling the El Niño-Southern Oscillation. Across the CCS, modes of upwelling variability are similar to one another, while modes differ between regions in the BCS. This difference could lead to regional mismatches in favorable ecological conditions. In contrast with the spatially synchronous winter variability influencing the entire CCS ecosystem, substantial regional variation in the BCS may have strong effects on ecosystem functions, especially for species (e.g., small pelagic fish) that migrate between the Agulhas Bank and other areas of the BCS.

Keywords

Upwelling Variability, Benguela Upwelling System, California Upwelling System, Upwelling Seasonality

Introduction

Seasonality is a ubiquitous feature of mid- and high-latitude terrestrial and aquatic ecosystems. In the coastal marine realm, in addition to changes in day length, seasons are often best characterized by changes in winds, stratification, and water temperature. In the major Eastern Boundary Upwelling Ecosystems (EBUE) of the world (California, Humboldt, Canary [Spain to northwestern Africa], and Benguela Currents), alongshore, upwelling-favorable winds generally peak in the warm season, but within these systems, a seasonal cycle may be less evident at lower latitudes (*Chavez and Messié, 2009*). Upwelling systems are disproportionately important to society as they cover a small percentage of the world's oceans, yet produce a significant portion of the globe's capture fisheries (*Mann, 2000; Rykaczewski and Checkley, 2008*). Understanding the seasonal dynamics of winds and the upwelling process that brings cold nutrient-rich waters to the surface to stimulate food web dynamics is therefore of great significance.

Long-term observational and modeling studies of the California Current System (CCS) have revealed large-scale variability in the seasonality of winds that is of key importance to regional ecology. In the CCS, upwelling-favorable winds exhibit variability that occurs in two distinct seasonal modes (*Black et al., 2011*), the first of which is a summer mode dominated by decadal-scale variability and an increasing linear trend in the northern CCS during the last several decades (*Sydeman et al., 2014*). The other is a winter mode dominated by higher-frequency variability driven by the positioning and strength of the North Pacific High (NPH) and teleconnections to the El Niño Southern-Oscillation (ENSO). Biological processes respond differently to these modes of upwelling variability, some of which track the winter pattern and others track the summer pattern. As interannual variability in the winter mode is especially pronounced, it has a strong synchronizing effect across trophic levels from copepod community composition to rockfish (*Sebastes*) growth, to seabird reproductive success (*Wells et al., 2008; Black et al., 2011; Thompson et al., 2012; García-Reyes et al., 2013b; Black et al., 2014*). Given the biological importance of seasonal upwelling winds in the CCS and the

sensitivity of these processes to global warming, we sought to explore if other major upwelling ecosystems in the world are similarly structured.

In this work, we hypothesize that similar patterns and drivers of upwelling-favorable winds are found in the Benguela Current System (BCS). While upwelling in both systems is driven by the pressure gradient between ocean high- and continental thermal low-pressure atmospheric systems, each EBUE has unique regional characteristics that could lead to unique properties of upwelling variability. The most important differences between these systems include i) the strong coupling of equatorial and North Pacific climate variability (*Di Lorenzo et al., 2013*) without an apparent analog in the South Atlantic (*Chang et al., 2006*); and ii) the presence of the warm and remotely driven Agulhas Current that bounds the poleward extent of the BCS in contrast to the subarctic, cold current (the North Pacific Current) that bounds the poleward extent of the CCS. The BCS is also more subtropical in reach, extending from 17° to 35°S, whereas the CCS stretches from about 30° to 48°N. Another difference is that the CCS coastline is oriented north to southeast while the BCS coastline is meridional, capped by a prominent zonal shift at Cape Agulhas along the southwestern coast of South Africa. In both systems, coastal upwelling is concentrated at capes and headlands in upwelling "cells" (*Checkley and Barth, 2009; Kirkman et al., 2016*), by winds that vary in synoptic - days to weeks - time scales (*Risien et al., 2004; García-Reyes et al., 2014*). In the CCS, upwelling-favorable winds are most persistent in the summer (*Dorman and Winant, 1995; García-Reyes and Largier, 2012*), when the North Pacific High is stable and extends along the entire system (*Schroeder et al., 2013*). In contrast, the South Atlantic High seasonal migration is small as the African continent ends at 34.5°N. As a result, the southern Benguela region is subjected to the influence of fronts and other mesoscale features leading to significant synoptic variability year-round (*Risien et al., 2004*).

To test if upwelling-favorable winds in the BCS occur in two distinct winter and summer modes of variability like in the CCS, attributable to the influence of regional climate forcing, we conducted a statistical decomposition of daily wind

fields at the regional scale in each system, from 1979 through 2014, and related the derived indicators of upwelling-favorable winds to atmospheric drivers, particularly the oceanic high-pressure systems. Resolving the similarities and differences in the seasonal variability of upwelling in the BCS and CCS is important to understanding and predicting potential changes to EBUE ecosystem productivity relative to long-term climate change.

Data & Methods

Study Region - In both the Benguela and California Current systems three regions are defined (Table 1, Figure 1). In the CCS: northern, central, and southern California regions, and in the BCS: northern and southern Benguela and Agulhas Bank regions - although the latter is not generally considered to be part of the BCS upwelling system, it has a large influence on the southern Benguela oceanographic and ecological conditions and therefore is included in this analysis. The BCS northern boundary was chosen at 14.75°S, fully covering the average location of the Angola Front (~17°S, *Hutchings et al., 2009*). See the Supplemental Material for a comparison of data from two definitions of the Northern Benguela region: one including and one excluding the Angola Front. In the following analyses, we used similar data and methodology in both systems to facilitate comparison.

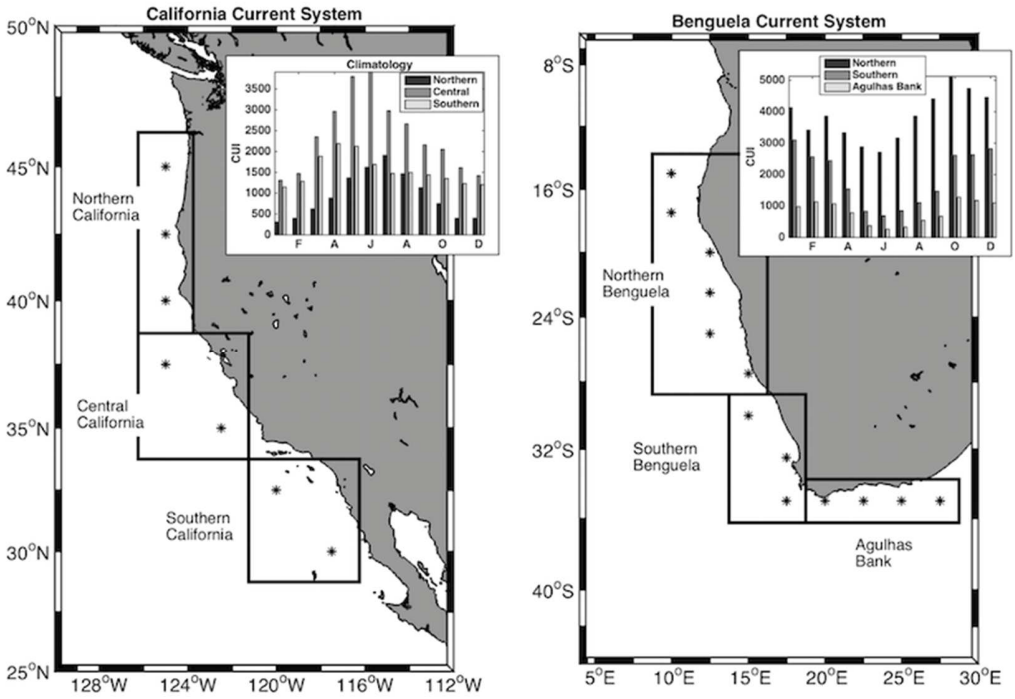

Figure 1. Maps of the California and Benguela Current Systems, indicating the regions of study and the center location of each NCEP2 data grid point (stars). Insets show the climatology of CUI for each region in each system.

System/Region	Latitude range	**PC1** (Eigen-value/explained variance)	**PC2** (Eigen-value/explained variance)
California System			
Northern	38.75-46.25°N	2.15 / 18%	2.05 / 17%
Central	33.75-38.75°N	2.38 / 20%	1.93 / 16%
Southern	28.75-33.75°N	2.07 / 17%	1.84 / 15%
Benguela System			
Northern	14.75-28.75°S	7.91 / 66%	0.88 / 7%
Southern	28.75-36.25°S	2.59 / 22%	1.62 / 14%
Agulhas Bank	18.25-28.25°E*	2.44 / 20%	1.73 / 14 %

Table 1. Latitudinal range and statistics of the principal component analysis (eigenvalues and explained variance) of the cumulative positive upwelling index (CUI) for each region in the California and Benguela systems. *Longitude range for Agulhas Bank.

Data.

Cumulative Upwelling Index – Following Lamont et al. (*this issue*), the monthly Cumulative Upwelling Index (CUI) was calculated as sum of daily positive Ekman transport, as a proxy to upwelling in both systems. Daily Ekman transport values were calculated from daily surface alongshore winds using the NCEP-DOE Reanalysis 2 data set (NCEP2, http://www.esrl.noaa.gov/psd/, June 2016; *Kanamitsu et al., 2002*), following Bakun (*1973*), from the period January 1979 to December 2014. This calculation places emphasis on upwelling by avoiding any situation in which negative Ekman transport values (downwelling) could cancel positive values within the same month, as would occur if means had been applied. CUI values at each NCEP2 grid point along the coast were then averaged by region (Table 1, Figure SM3). Each regional time series was linearly detrended to remove potential trends that may obscure the seasonal modes of variability in these relatively short time series (*Sydeman et al., 2014; Lamont et al., this issue*). The

NCEP2 dataset was chosen over other longer reanalysis datasets because it provides the most consistent, up-to-date, high temporal frequency across both systems (*Kent et al., 2013; Lamont et al., this issue*).

Atmospheric data – To investigate potential drivers of the seasonal modes of variability, we compared the derived upwelling-favorable wind modes to indices that track variability in the magnitude and positioning of the mid-latitude oceanic high-pressure systems (OHPS) the driving force of winds in these systems (*García-Reyes et al., 2013a*): North Pacific High (hereafter NPH) for the CCS and South Atlantic High (hereafter SAH) for the BCS. These indices were calculated from NCEP2 sea level pressure (SLP) data, following the methodology of Schroeder et al. (*2013*). From the SLP climatology, 1020 and 1018 hPa isobars were selected to delimit the NPH and the SAH, respectively (the SAH has, on average, lower SLP values). For each season, the mean SLP of all points within this isobar was calculated as an index of magnitude, while position (NPHx, NPHy, SAHx, SAHy) was calculated as the average latitude and longitude of each point inside the isobar weighted by its SLP value. In addition, we compared modes of wind variability with SLP and sea surface temperature (SST) fields from Met Office Hadley Center observations datasets (HadISST 1° and HadSLP2 5°, respectively; http://metoffice.gov.uk, November 2016; *Rayner et al., 2003; Allan and Ansell, 2006*).

Methodology

All of the time series, including the global SLP and SST data, were linearly detrended for comparison with CUI data. Within each region, Principal Component Analysis (PCA) was performed on monthly-averaged CUI anomaly time series, following the methods of Black et al. (*2011*). Each detrended time series was normalized and then redistributed in a matrix with 12 columns corresponding to each month and 36 rows corresponding to each year. We used two main criteria to identify seasonal modes: i) a clear and coherent pattern of high principal component (PC) monthly coefficients and high autocorrelation spanning a few consecutive months, and ii) a significant ($p < 0.05$) rank correlation between the PC and at least one seasonal mean of CUI. Seasons were defined in quarterly (3-month) periods

191 with January-March as winter for the California Current, and July-September as
192 winter for Benguela Current. This second criteria not only serves as an indicator of
193 the physical interpretation of the PC, but also tests its validity as a unique PC when
194 PC1 and PC2 have similar eigenvalues. In addition, explained variance (eigenvalues)
195 of the principal components was considered when selecting the relevant mode of
196 variability. These criteria identified strong seasonal modes of variability and helped
197 exclude modes driven by a few extreme values in the data.
198 To explore potential drivers of the modes of variability within and across
199 systems, we: i) cross-correlated the modes scores (time series) within and across
200 the California and Benguela systems, and ii) correlated the modes scores (time
201 series) with indices of the OHPS (NPH, SAH), SLP, and SST data fields. For (ii), three-
202 month (seasonal) averages of monthly data (OHPS, SLP or SST) were calculated and
203 then lag-correlated (rank correlation, $p < 0.05$) by season with the modes scores.
204 We also investigated covariability in upwelling between systems. For this we
205 performed a cross-wavelets analysis on modes across systems as well as a PCA of
206 the summer upwelling modes across both systems. This resultant PC ($PC_{upwelling}$)
207 was also correlated to SLP and SST fields.
208
209 **Results**
210 *Modes of variability*
211 As expected, the CCS shows two seasonal modes of upwelling-favorable wind
212 variability, which are similar in all regions. PCA loadings (monthly coefficients) are
213 shown in Figure 2, scores are shown in Figure SM6, and the eigenvalues and
214 explained variances are given in Table 1. The leading mode of variability (PC1) is
215 focused on winter and early spring (Figure 2a) for the northern and central regions,
216 and winter and spring for the southern region. These leading PCs correlate the
217 strongest with winter CUI (Figure 3), especially in the north, while the southern
218 region PC1 also correlates well with spring. In the CCS, the central region PC1 is the
219 strongest (explains 20% of the variability). The second principal component (PC2)
220 has a somewhat similar seasonal pattern in all CCS regions: central and northern
221 California PC2 show a seasonal signature focused on spring and summer, while

southern California PC2 is focused only in spring, all coincident with the climatological peak of upwelling in these regions (Inset in Figure 1). However, both central and southern California PC2 modes are weaker than in the north, as evidenced by lower eigenvalues and lower correlations to seasonal CUI. In the northern region, eigenvalues for PC1 and PC2 are similar, prompting the question: are both PCs the same (degenerate)? However, the significant correlation of each PC with different seasons of CUI values indicates that they are indeed different PCs and independent of each other. In the southern region, the PC2 time series has weak autocorrelation across adjacent months (Figure SM4).

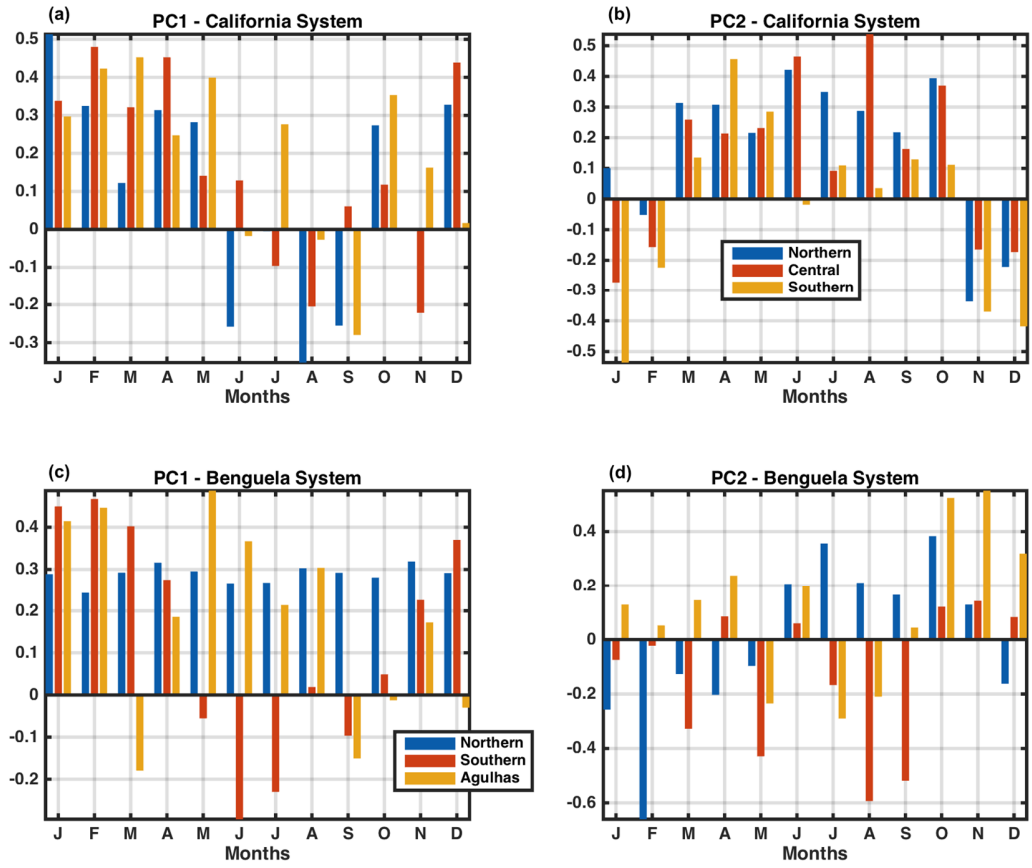

Figure 2. Loadings (coefficients) of the Principal Component Analysis for monthly cumulative upwelling index (CUI) for the different California and Benguela System regions.

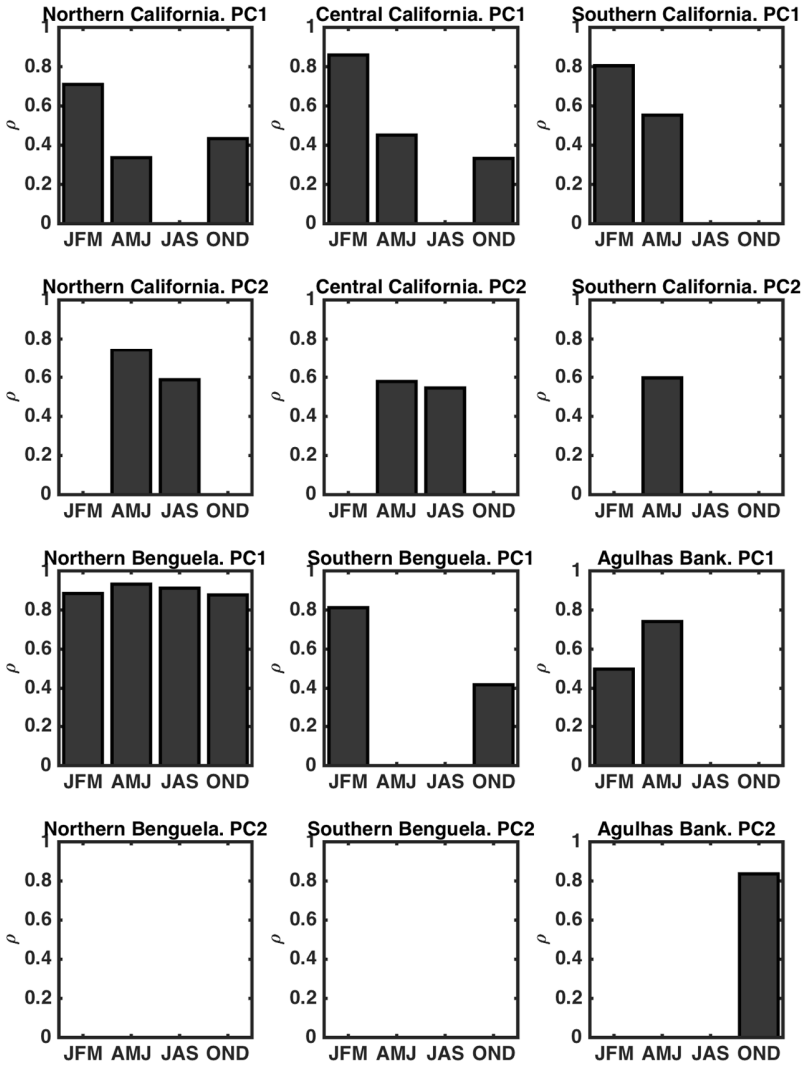

Figure 3. Rank correlations between modes of variability (PCs time series) and seasonal means of CUI for each system and each region. Only significant ($p < 0.05$) correlations are shown, and all values are positive to facilitate comparison. No adjustment for autocorrelation was performed.

The BCS has greater differences between regions in seasonal modes of upwelling than the CCS. The northern and southern Benguela regions exhibit only one mode of upwelling variability. The northern Benguela PC1 is strong, capturing two thirds of the variability in CUI (Table 1), but shows no seasonality. This is evidenced by the strong autocorrelation across months (Figure SM5), the fact that PC1 coefficients are similar in each month of the year (Figure 2c, blue), as are the correlations between PC1 and the seasonal CUI averages (Figure 3). The second

principal component (PC2) is weak, explaining only 7% of the variance, with a dominant coefficient in February but weak correlations with seasonal CUI. The southern Benguela also shows only one mode that explains 22% of the variability but is focused (and correlated to CUI) in the austral summer (DJF), the peak of the upwelling season in this region (Figure 1). The second mode, though with a winter signature (peak correlations with August and September in Figure 2d), is not significantly correlated with winter CUI (Figure 3). The Agulhas Bank region has two independent seasonal modes of variability: PC1 loads from summer to mid-winter and correlates significantly with fall CUI averages (Figure 3). The second PC is focused in spring (October-December) and has a significant and strong correlation with spring CUI averages, although with a low eigenvalue and weak autocorrelation (mode highly focused in spring).

In summary, the northern and central California and the Agulhas Bank regions show two independent seasonal modes of variability. In the CCS, PC1 is dominant in winter-early spring and PC2 in spring-summer, while in the Agulhas Bank region PC1 dominates in summer-fall and PC2 prevails in spring. Southern California shows a strong PC1 in winter-spring, but a less clearly defined second mode, correlated with spring CUI. In the BCS, modes of variability are different among regions: northern Benguela shows no seasonal modes of variability, but one annual mode, while the southern Benguela shows one mode of seasonal variability that captures the upwelling season.

There is some coherence in modes across the study region, though it is not always consistent. In the CCS, PC1 scores are significantly correlated only between the northern and central regions ($\rho = 0.71$, $p < 0.001$, Figure SM5). PC2 scores also covary across the central and northern regions ($\rho = 0.74$, $p < 0.001$), but they are not significantly correlated with the southern region. Central and northern California PC2 have a decadal pattern not observed in the southern California PC2 or in PC1 for any region. In the BCS, the only significant correlations, although weak, are between the northern and southern PC1s ($\rho = 0.36$, $p < 0.05$), as well as the southern Benguela and Agulhas Bank PC2s ($\rho = 0.44$, $p < 0.01$).

Drivers of modes of variability

Modes of variability (PCs) correlate moderately with the magnitude and location of the OHPS, except for the southern Benguela PC1 and southern California PC2, which do not consistently correlate with any measure of the OHPS (Table 2). The strongest and most consistent relationships with OHPS occur for the California winter modes (PC1), especially in the northern and central regions. Notably, the CCS (PC1) and BCS (PC2) share the same seasonality (January-March) in their correlations with OHPS magnitude.

System/Region/Mode	Magnitude	Latitude	Longitude
California PC1			
Northern California	0.64 (Jan-Mar)	0.53 (Jan-Mar)	-0.40* (Jul-Sep)
Central California	0.70 (Jan-Mar)	0.53 (Jan-Mar)	-0.38* (Jul-Sep)
Southern California	0.36* (Jan-Mar)	-0.57 (Oct-Dec)	-
California PC2			
Northern California	0.39* (Apr-Jun)	-0.41* (Oct-Dec)	-
Central California	-	-0.38* (Oct-Dec)	-
Southern California	-	-	-
Benguela PC1			
Northern Benguela	-	-	-0.42* (Jul-Sep)
Southern Benguela	-	-	-
Agulhas Bank	-0.38* (Jul-Sep)	-0.56 (Jan-Mar)	0.37* (Jan-Mar)
Benguela PC2			
Northern Benguela	-0.43 (Jan-Mar)	-	0.44 (Oct-Dec)
Southern Benguela	-0.33* (Jan-Mar)	-0.44 (Oct-Dec)	-
Agulhas Bank	-0.49 (Apr-Jun)	-0.51 (Oct-Dec)	-

Table 2. Rank correlations (ρ) between modes of upwelling variability in the California Current System (CCS) and Benguela Current System (BCS) and the magnitude and position (latitudinal and longitudinal) of the regional ocean high-pressure systems. Seasons with the highest significant correlations ($p < 0.01$, * for $p < 0.05$) are shown in parentheses.

To further explore the source of the variability in the modes of upwelling, we calculated correlations between the scores of the modes and SLP and SST fields. The summer modes of variability (northern California PC2, central California PC2, and southern Benguela PC1) are not well correlated with SLP fields except in the subpolar regions (Figure SM7). SST correlations are even less significant, but all modes do have positive correlations with a small region in the north Atlantic (Figure SM7). The winter modes of the three California regions are all significantly correlated with North Pacific SLP in a region around the climatological location of

the NPH (Figure 4). Correlations for central California PC1 are similar to those for northern California PC1,(data not shown). The northern and central California PC1s correlate with northeast Pacific SST in an arc pattern that resembles the Pacific Decadal Oscillation (PDO, *Mantua and Hare, 2002*), and the southern California PC1 correlates with a band in the tropical eastern Pacific (Figure 4). The Agulhas Bank PC1 is highly correlated to equatorial conditions, largely in the Pacific, suggesting sensitivity to ENSO. A significant and positive correlation with seasonal averages of the Southern Oscillation Index (SOI, not shown) confirms the influence of ENSO on the Agulhas Bank first mode of upwelling variability.

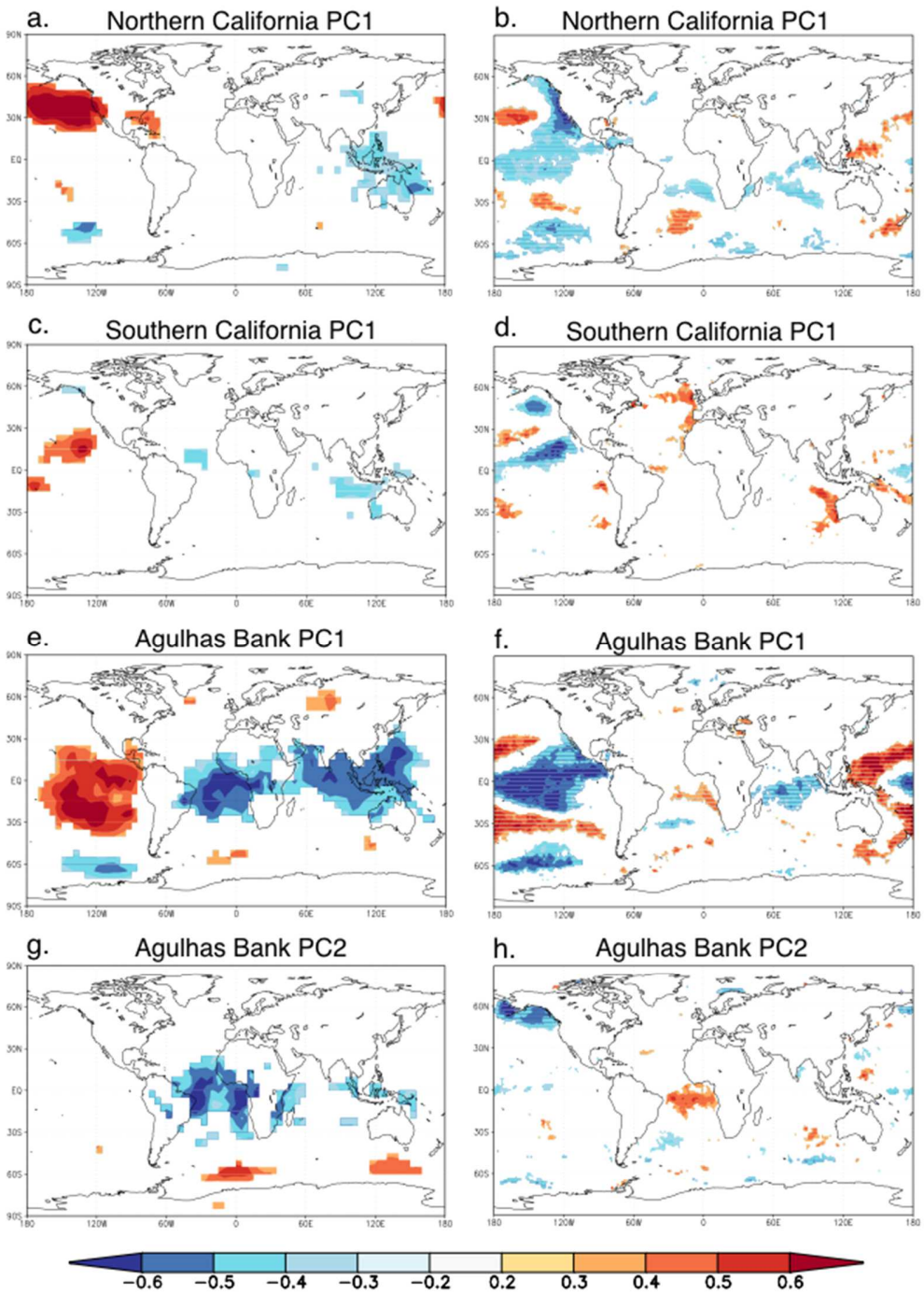

Figure 4. Rank correlations between seasonal upwelling modes of variability and 3-month average sea level pressure (HadSLP2) and SST fields (HadISST1) ($p < 0.05$ shown) for the period 1979-2014. Northern California PC1 with (a) Jan.-Mar. SLP and (b) Jan.-Mar. SST; Southern California PC1 with (c) Feb.-Apr. SLP and (d) Feb.-Apr. SST; Agulhas Bank PC1 with (e) Jan.-Mar. SLP and (f) Feb.-Apr. SST; and Agulhas Bank PC2 with (g) Jun.-Aug. SLP and (h) May-Jul. SST.

322

323 *Shared variability in upwelling modes between systems*

324 In comparing modes across systems, there are 4 significant correlations:
325 Agulhas Bank PC1 and central California PC2 (ρ = 0.34); southern Benguela PC2
326 with southern California PC2 (ρ = 0.35), northern California PC2 and southern
327 Benguela PC1 (ρ = 0.34), and central California PC2 with southern Benguela PC1 (ρ
328 = 0.36). Thus, the majority of coherence was between summer wind modes. To
329 explore the periodicity of shared variability, we performed a cross-wavelets analysis
330 (Figure 5), which shows covariability among the three summer PCs, particularly at
331 periods around 8 years with the greatest power later in the study period. It also
332 shows covariability at 1- to 2-year periods, particularly after 1990. Notably, the
333 northern California and southern Benguela summer modes show strong
334 covariability in most frequencies from the early 1990s to the end of the record. A
335 PCA of the three summer modes (Figure 6; $PC_{upwelling}$) explains 66% of the variability
336 in the upwelling modes, largely due to shared decadal-scale variability. Loadings for
337 $PC_{upwelling}$ are 0.59 for northern California PC2, 0.64 for central California PC2 and
338 0.49 for southern Benguela PC1. The correlations of $PC_{upwelling}$ with SLP and SST
339 fields show a similar signature as the individual summer modes (Figure SM7,
340 bottom): positive correlations over in the Arctic and Greenland, and negative
341 correlations with northeast Africa and eastern Europe. With respect to SST,
342 negative correlations also occur over the North Atlantic. It is worth noting that
343 similar correlations occur when other SLP and SST datasets are used (Figure SM8).
344

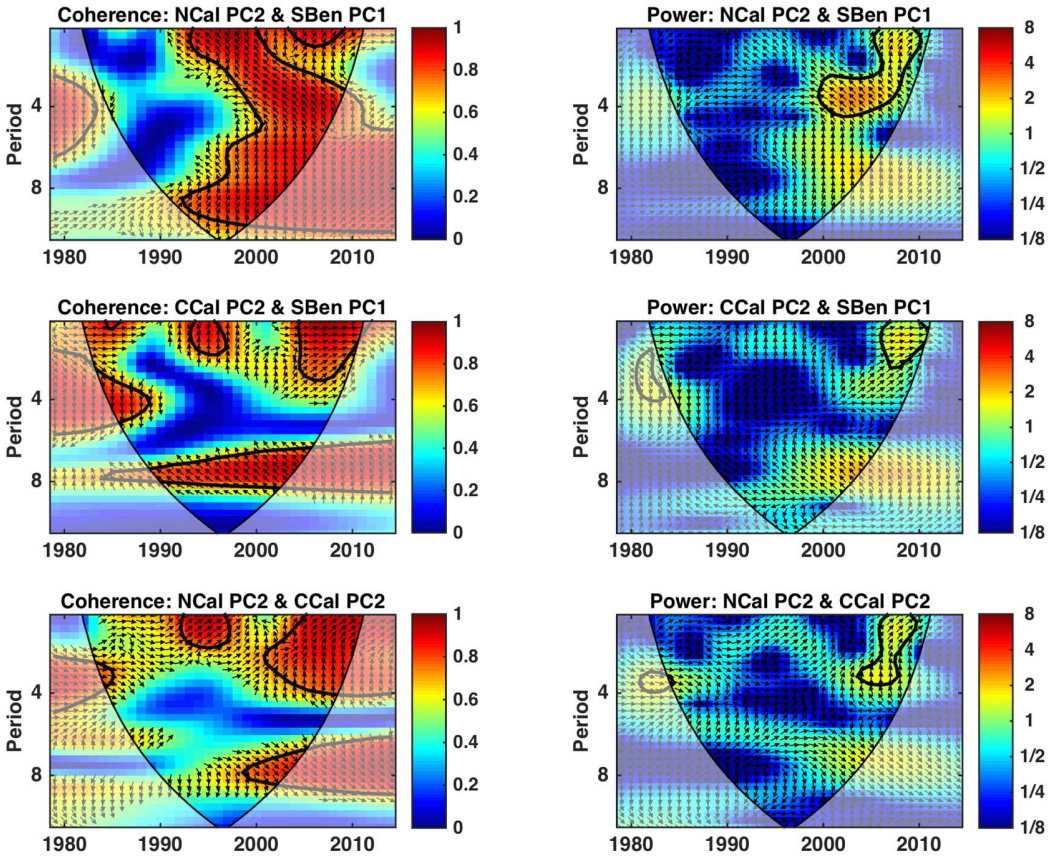

Figure 5. Cross-wavelet analysis between summer upwelling modes: northern California PC2 (NCal), central California PC2 (CCal), and southern Benguela PC1 (SBen). Left plots show the cross-wavelet coherence and right plots show the power.

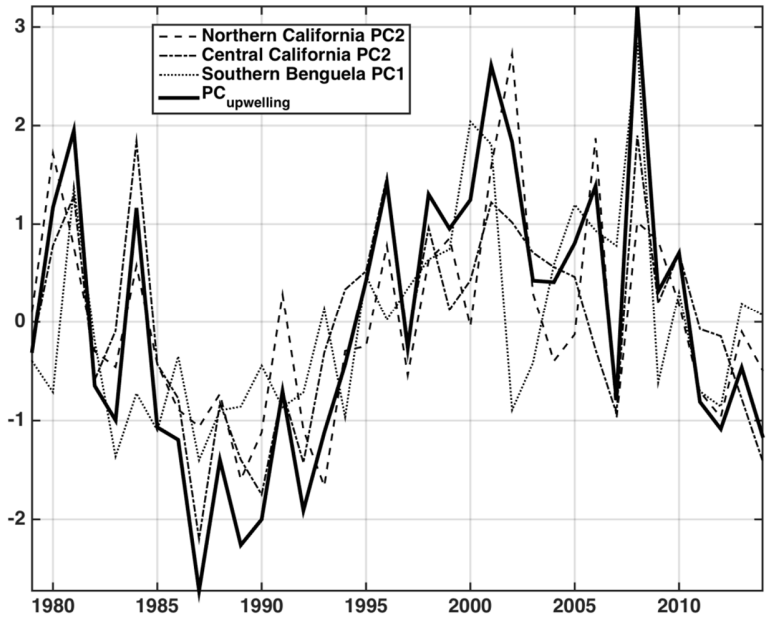

Figure 6. First PC ($PC_{upwelling}$) of the summer upwelling modes (heavy black line): northern and central California PC2 and southern Benguela PC1.

Discussion

Consistent with findings of Black et al. (*2011; 2014*), we found two independent seasonal modes of wind variability in the CCS. In the northern and southern Benguela, however, only one mode of variability was derived, which is year-round in the north and spans the peak of the upwelling season (summer) in the south. Notably, the Agulhas Bank region has two upwelling modes, one focused on fall and another on spring. Seasonal modes are more coherent across regions in the CCS than the BCS. The CCS is best characterized by a winter mode and a spring and/or summer mode depending on the region, whereas the BCS is best characterized by an annual mode, a summer mode, and fall and spring modes.

In both systems, although not in all regions, there are seasonal modes of variability that represent the primary upwelling season. In the southern Benguela, this is the leading mode of variability, while in the northern and central California it is the second mode. In the most equatorward regions, northern Benguela and

369 southern California, upwelling occurs all year, which could explain the lack of
370 seasonal modes in the northern Benguela and lack of strong seasonality in southern
371 California.
372 The summer upwelling modes (northern and central California PC2 and
373 southern Benguela PC1) have similar patterns of decadal variability. Although the
374 length of the NCEP2 dataset is not optimal for characterizing decadal variability, the
375 observed decadal variability in the summer modes is consistent with the variability
376 of the summer upwelling mode presented by Black et al. (*2011*); this mode is
377 characterized by low values in the late 1980s that increase through the 1990s and
378 decrease again in the late 2000s. Similar decadal variability in summer upwelling
379 has also been reported by Mendelssohn and Schwing (*2002*) and Macias et al. (*2012*)
380 for the CCS, and Narayan et al. (*2010*) and Blamey et al. (*2012*) for the BCS. Jarre et
381 al. (*2015*) suggested that decadal variability observed in the BCS summer upwelling
382 is related to the variability in the latitudinal position of the SAH. In our analysis,
383 summer upwelling correlates with the magnitude and position of the OHPS in the
384 northern and central CCS, and in the northern and Agulhas Bank regions of the BCS.
385 However, due to the short length of the time series and removal of long-term trends,
386 this correlation is attributable mainly to inter-annual variability. A cross-wavelet
387 analysis between summer modes and summer latitudinal position of the OHPS
388 shows coherence only for the central California summer mode (PC2) and the NPHy
389 at decadal time scales (not shown). Unfortunately, for these relatively low
390 frequencies, the significance of the results is limited by the length of the time series
391 (cone of influence). However, the entirety of our analysis does indicate that the
392 magnitude and location of the OHPS are important to summer upwelling. This is of
393 importance for forecasting future patterns of summer upwelling considering that
394 global circulation models (*Rykaczewski et al., 2015; Wang et al., 2015*) suggest global
395 climate change will shift the latitude of the four OHPS poleward.
396 Shared patterns in the summer upwelling modes across the BCS and CCS
397 represent only 10-15% of the total variability in the CUI time series, but it does
398 suggest that global-scale processes may influence upwelling-favorable winds in
399 these EBUE. The cross-wavelets power analysis suggests that this shared variability

400 operates largely on decadal scales and it is more tightly coupled in recent decades.
401 The 1- to 2-year variability observed in the cross-wavelets, however, is less stable
402 over time and may reflect random processes. Investigating the forcing of this
403 covariability is beyond the scope of this paper, however, $PC_{upwelling}$ positively
404 correlates to SLP and SST fields in the Arctic and Greenland, and negatively in west
405 Africa/Europe. A similar correlation pattern occurs when using multiple SLP
406 datasets (Figure SM8), which suggests that this result is not an artifact of the NCEP2
407 dataset. There is however, no immediate explanation for these correlation fields.
408 In contrast to summer, the winter upwelling variability modes in the three
409 CCS regions (PC1) and the southern Benguela PC2 correlate at interannual scales to
410 the magnitude and latitudinal position of the oceanic high-pressure systems. This is
411 consistent with previous results showing that winter winds are better related to the
412 OHPS variability than summer winds (*García-Reyes et al., 2013a)*, as the OHPS tend
413 to be stable during the summer (*IPCC, 2013 Fig. 2.37; Schroeder et al., 2013*).
414 Furthermore, in the CCS, the winter mode is strongly correlated with regional SLP
415 and SST fields in a pattern consistent with the PDO. Additionally, some negative
416 correlation with the western equatorial Pacific SLP is observed with the northern
417 and central California winter modes, suggesting some influence from equatorial
418 atmospheric teleconnections. Previous studies have shown the influence of Pacific
419 teleconnections on northeastern Pacific atmospheric patterns, including winter
420 winds (for example, see *Schwing et al., 2002*).
421 However, in the south Atlantic there are no correlations with regional
422 atmospheric patterns to the degree found in the Pacific. Infrequent climate events
423 dubbed Benguela Niños occur (*Shannon et al., 1986*), but they have a less clear and
424 coherent atmospheric signature in the Atlantic than Pacific El Niños do in the Pacific.
425 Variability in the Indian Ocean pressure fields and the Southern Annular Mode
426 (SAM) have been reported to influence the BCS as well (*Hutchings et al., 2009;*
427 *Reason et al., 2013)*, but the SST field correlations did not suggest clear influence
428 from the Indian Ocean or the Antarctic. Similarly, we did not find clear correlations
429 between the equatorial Pacific and the BCS seasonal modes (PC1), which would
430 have suggested ENSO as a driver for this leading mode. However, some moderate

431 correlations between ENSO and the second mode of variability in the BCS (not
432 shown) suggest that ENSO events do influence upwelling in the BCS as suggested by
433 other authors (*Colberg et al., 2004; Rouault et al., 2010; Tim et al., 2013*). It is likely
434 that because ENSO activity peaks during the Southern Hemisphere summer, which
435 is when the SAH and adjacent land pressure system are most stable and upwelling is
436 strong, only certain ENSO events show visible signatures. Rouault et al. (*2010*) also
437 discussed how the contrasting simultaneous impacts of ENSO and SAM could mask
438 their signatures on SSTs in the BCS.
439 Interestingly, in the results of this study, winter was identified as the leading
440 mode of variability in the CCS. Black et al. (*2011*), in a similar analysis based on the
441 Bakun upwelling index (*Bakun, 1973*), found the California winter mode to be
442 second to a summer mode of variability in the summer. In the analysis by Black et al.
443 (*2011*), using data from 1948 to 2010, the winter mode scores appear to be higher
444 in the latter half of the time period, which corresponds to the period of this analysis
445 (1979-2014). The lower scores (and variance) in the first half could be the reason
446 for the winter mode to be the second mode of variability in their analysis, but first in
447 ours, also suggesting increasing variability in winter upwelling (*Black et al., 2014*).
448 The Agulhas Bank region was included in this analysis because it is a coastal
449 upwelling area that is ecologically relevant (a spawning region for small pelagic
450 fishes) for the Benguela Current ecosystem given the transport of water masses
451 around Cape Agulhas into the BCS (*Colberg et al., 2004; Boschat et al., 2013; Blamey*
452 *et al., 2015*). Notably, its leading mode of variability occurs in the summer-fall
453 (January-June), while the peak of upwelling is in spring-summer (October-March).
454 This is most likely due to the influence of the ENSO teleconnections, as the ENSO
455 influence on zonal winds at this latitude is strongest during the austral summer and
456 subsequent season (*L'Heureux and Thompson, 2006)*. This is supported by the
457 strong correlation found between the Agulhas Bank first mode of upwelling
458 variability with Pacific equatorial SLP in summer and fall. The Agulhas Bank second
459 mode correlations with SLP and SST fields (Figure 4) resemble a pattern related to
460 the Atlantic zonal mode (*Zebiak, 1993*).

In the CCS, the existence of two independent modes of upwelling variability has important ecological implications, as each mode impacts different components of the marine ecosystem. In particular, the highly variable winter upwelling and associated conditions have a synchronizing effect across trophic levels in the California marine ecosystem (*Black et al., 2011; Thompson et al., 2012*), which extends to adjacent terrestrial species (*Black et al., 2014*). Schroeder et al. (*2009*) proposed that winter upwelling-favorable events pre-condition the coastal ecosystem by stimulating an early onset of a nutrient-rich environment (*Chavez et al., 2011*) and primary productivity (*Holt and Mantua, 2009*). An important difference between these two systems is that in the BCS there is no single seasonal mode of upwelling variability that could have the synchronizing effect that winter does in the CCS, although isolated extreme events might have this effect occasionally. Another difference is the spatial heterogeneity in seasonal modes among regions in the BCS. This could be particularly important for the southern Benguela and Agulhas Bank regions since they are linked not only physically, but also biologically as a number of species spend crucial parts of their lives on each side of Cape Agulhas (summarized in *Hutchings et al., 2009*). Incoherent periods of favorable or unfavorable conditions could occur if upwelling modes independently vary in timing or magnitude between these two regions, which could affect ecosystem productivity and structure of this region. Comparative analyses that consider the existence/lack of synchronizing events and the in-phase/out-of-phase variability in EBUE are necessary to test their importance in influencing regional to macroscale functions in these ecosystems.

Acknowledgements

NCEP-DOE Reanalysis 2 data was provided by the NOAA/OAR/ESRL PSD, Boulder, Colorado, USA (http://www.esrl.noaa.gov/psd/). The authors thank Cayley Geffen for her support with the graphics. MGR, WJS, BAB, RRR, SAT, and SJB were funded by the National Science Foundation award No: OCE-1434732. TL thanks the Department of Environmental Affairs (DEA) and the Department of Agriculture, Forestry and Fisheries (DAFF), South Africa for funding and facilities.

References

1. Allan, R., & Ansell, T. (2006). A new globally complete monthly historical gridded mean sea level pressure dataset (HadSLP2): 1850-2004. *Journal of Climate*, *19*(22), 5816-5842. doi: 10.1175/JCLI3937.1
2. Bakun, A. (1973), Coastal upwelling indices, west coast of North America, 1946–71, *NOAA Tech. Rep. NMFS SSRF, 671*, 103 pp.
3. Black, B. A., Schroeder, I. D., Sydeman, W. J., Bograd, S. J., Wells, B. K., & Schwing, F. B. (2011). Winter and summer upwelling modes and their biological importance in the California Current Ecosystem. *Global Change Biology*, *17*(8), 2536-2545. doi: 10.1111/j.1365-2486.2011.02422.x
4. Black, B. A., Sydeman, W. J., Frank, D. C., Griffin, D., Stahle, D. W., García-Reyes, M., ... & Peterson, W. T. (2014). Six centuries of variability and extremes in a coupled marine-terrestrial ecosystem. *Science*, *345*(6203), 1498-1502. doi: 10.1126/science.1253209
5. Blamey, L. K., Howard, J. A., Agenbag, J., & Jarre, A. (2012). Regime-shifts in the southern Benguela shelf and inshore region. *Progress in Oceanography*, *106*, 80-95. doi: 10.1016/j.pocean.2012.07.001
6. Blamey, L. K., Shannon, L. J., Bolton, J. J., Crawford, R. J., Dufois, F., Evers-King, H., ... & Watermeyer, K. E. (2015). Ecosystem change in the southern Benguela and the underlying processes. *Journal of Marine Systems*, *144*, 9-29. doi: 10.1016/j.jmarsys.2014.11.006
7. Boschat, G., Terray, P., & Masson, S. (2013). Extratropical forcing of ENSO. *Geophysical Research Letters*, *40*(8), 1605-1611. doi: 10.1002/grl.50229
8. Chang, P., Yamagata, T., Schopf, P., Behera, S. K., Carton, J., Kessler, et al. (2006). Climate fluctuations of tropical coupled systems—the role of ocean dynamics. *Journal of Climate*, *19*(20), 5122-5174. doi: 10.1175/JCLI3903.1
9. Chavez, F. P., & Messié, M. (2009). A comparison of eastern boundary upwelling ecosystems. *Progress in Oceanography*, *83*(1), 80-96. doi: 10.1016/j.pocean.2009.07.032
10. Chavez, F. P., Messié, M., & Pennington, J. T. (2011). Marine primary production in relation to climate variability and change. *Annual Review of Marine Science*, *3*, 227-260. doi: 10.1146/annurev.marine.010908.163917
11. Checkley, D. M., & Barth, J. A. (2009). Patterns and processes in the California Current System. *Progress in Oceanography*, *83*(1), 49-64. doi: 10.1016/j.pocean.2009.07.028
12. Colberg, F., Reason, C. J. C., & Rodgers, K. (2004). South Atlantic response to El Niño–Southern Oscillation induced climate variability in an ocean general circulation model. *Journal of Geophysical Research: Oceans*, *109*(C12). doi: 10.1029/2004JC002301
13. Di Lorenzo, E., Combes, V., Keister, J.E. & … (2013) Synthesis of Pacific Ocean climate and ecosystem dynamics. *Oceanography, 26*(4), 68-81. doi: 10.5670/oceanog.2013.76

14. Dorman, C. E., & Winant, C. D. (1995). Buoy observations of the atmosphere along the west coast of the United States, 1981-1990. *Journal of Geophysical Research, 100*, 16-029. doi: 10.1029/95JC00964
15. García-Reyes, M., & Largier, J. L. (2012). Seasonality of coastal upwelling off central and northern California: New insights, including temporal and spatial variability. *Journal of Geophysical Research: Oceans*, *117*(C3). doi: 10.1029/2011JC007629
16. García-Reyes, M., Sydeman, W. J., Black, B. A., Rykaczewski, R. R., Schoeman, D. S., Thompson, S. A., & Bograd, S. J. (2013a). Relative influence of oceanic and terrestrial pressure systems in driving upwelling-favorable winds. *Geophysical Research Letters*, *40*(19), 5311-5315. doi: 10.1002/2013GL057729
17. García-Reyes, M., Sydeman, W. J., Thompson, S. A., Black, B. A., Rykaczewski, R. R., Thayer, J. A., & Bograd, S. J. (2013b). Integrated assessment of wind effects on central California's pelagic ecosystem. *Ecosystems*, *16*(5), 722-735. doi: 10.1007/s10021-013-9643-6
18. García-Reyes, M., Largier, J. L., & Sydeman, W. J. (2014). Synoptic-scale upwelling indices and predictions of phyto-and zooplankton populations. *Progress in Oceanography*, *120*, 177-188. doi: 10.1016/j.pocean.2013.08.004
19. Holt, C. A., & Mantua, N. (2009). Defining spring transition: regional indices for the California Current System. *Marine Ecology Progress Series*, *393*, 285-299. doi: 10.3354/meps08147
20. Hutchings, L., Van der Lingen, C. D., Shannon, L. J., Crawford, R. J. M., Verheye, H. M. S., Bartholomae, C. H., ... & Fidel, Q. (2009). The Benguela Current: An ecosystem of four components. *Progress in Oceanography*, *83*(1), 15-32. doi: 10.1016/j.pocean.2009.07.046
21. IPCC (2013): Climate Change 2013: The Physical science Basis. Contribution of Working Group I to the Fifth Assessment Report of the Intergovernmental Panel on Climate Change [Stocker, T.F. et al. (eds.)]. *Cambridge University Press, Cambridge,* U.K. and New York, NY, USA. 1535pp.
22. Jarre, A., Hutchings, L., Kirkman, S. P., Kreiner, A., Tchipalanga, P., Kainge, P., ... & Lamont, T. (2015). Synthesis: climate effects on biodiversity, abundance and distribution of marine organisms in the Benguela. *Fisheries Oceanography*, *24*(S1), 122-149. doi: 10.1111/fog.12086
23. Kanamitsu, M., Ebisuzaki, W., Woollen, J., & Shi-Keng, Y. (2002). NCEP-DOE AMIP-II reanalysis (r-2). *Bulletin of the American Meteorological Society*, *83*(11), 1631. doi: 10.1175/BAMS-83-11-1631
24. Kent, E. C., S. Fangohr, and D. I. Berry (2013). A comparative assessment of monthly mean wind speed products over the global ocean. *International Journal of Climatology, 33*, 2520-2541. doi: 10.1002/joc.3606
25. Kirkman, S. P., Blamey, L., Lamont, T., Field, J. G., Bianchi, G., Huggett, J. A., ... & Lipiński, M. R. (2016). Spatial characterisation of the Benguela ecosystem for ecosystem-based management. *African Journal of Marine Science*, *38*(1), 7-22. doi: 10.2989/1814232X.2015.1125390
26. Lamont, T., M. García-Reyes, S. J. Bograd, C.D. van der Lingen, W. J. Sydeman (*in press, this issue*) Upwelling indices for comparative ecosystem studies: variability in the Benguela Upwelling System. *Journal of Marine Sciences.*

27. L'Heureux, M. L., & Thompson, D. W. J. (2006). Observed relationship between the El Niño-Southern Oscillation and the extratropical zonal-mean circulation. *Journal of Climate, 19*, 276-287. doi: 10.1175/JCLI3617.1
28. Mann, K.H. (2000) *Ecology of Coastal Waters, With Implications for Management*, Blackwell Sci., Malden, Mass.
29. Mantua, N. J., & Hare, S. R. (2002). The Pacific decadal oscillation. *Journal of Oceanography*, *58*(1), 35-44. doi: 10.1023/A:1015820616384
30. Macias, D., Landry, M. R., Gershunov, A., Miller, A. J., & Franks, P. J. (2012). Climatic control of upwelling variability along the western North-American coast. *Plos One*, *7*(1), e30436. doi: 10.1371/journal.pone.0030436
31. Mendelssohn, R., & Schwing, F. B. (2002). Common and uncommon trends in SST and wind stress in the California and Peru–Chile current systems. *Progress in Oceanography*, *53*(2), 141-162. doi: 10.1016/S0079-6611(02)00028-9
32. Narayan, N., Paul, A., Mulitza, S., & Schulz, M. (2010). Trends in coastal upwelling intensity during the late 20th century. *Ocean Science*, *6*(3), 815-823. doi: 10.5194/os-6-815-2010
33. Rayner, N. A., Parker, D. E., Horton, E. B., Folland, C. K., Alexander, L. V., Rowell, D. P., ... & Kaplan, A. (2003). Global analyses of sea surface temperature, sea ice, and night marine air temperature since the late nineteenth century. *Journal of Geophysical Research: Atmospheres*, *108*(D14), 4407. doi: 10.1029/2002JD002670
34. Reason, C. J. C., Florenchie, P., Rouault, M., & Veitch, J. (2006). Influences of large scale climate modes and Agulhas system variability on the BCLME region. *Large Marine Ecosystems*, *14*, 223-238. doi: 10.1016/S1570-0461(06)80015-7
35. Risien, C. M., Reason, C. J. C., Shillington, F. A., & Chelton, D. B. (2004). Variability in satellite winds over the Benguela upwelling system during 1999–2000. *Journal of Geophysical Research: Oceans*, *109*(C3). doi: 10.1029/2003JC001880
36. Rouault, M., Pohl, B., & Penven, P. (2010). Coastal oceanic climate change and variability from 1982 to 2009 around South Africa. *African Journal of Marine Science*, *32*(2), 237-246. doi: 10.2989/1814232X.2010.501563
37. Rykaczewski, R. R., & Checkley, D. M. (2008). Influence of ocean winds on the pelagic ecosystem in upwelling regions. *Proceedings of the National Academy of Sciences*, *105*(6), 1965-1970. doi: 10.1073/pnas.0711777105
38. Rykaczewski, R. R., Dunne, J. P., Sydeman, W. J., García-Reyes, M., Black, B. A., & Bograd, S. J. (2015). Poleward displacement of coastal upwelling-favorable winds in the ocean's eastern boundary currents through the 21st century. *Geophysical Research Letters*, *42*(15), 6424-6431. doi: 10.1002/2015GL064694
39. Schroeder, I. D., Sydeman, W. J., Sarkar, N., Thompson, S. A., Bograd, S. J., & Schwing, F. B. (2009). Winter pre-conditioning of seabird phenology in the California Current. *Marine Ecology Progress Series*, *393*, 211-223. doi: 10.3354/meps08103
40. Schroeder, I. D., Black, B. A., Sydeman, W. J., Bograd, S. J., Hazen, E. L., Santora, J. A., & Wells, B. K. (2013). The North Pacific High and wintertime pre-conditioning of California current productivity. *Geophysical Research Letters*, *40*(3), 541-546. doi: 10.1002/grl.50100

41. Shannon, L. V., Boyd, A. J., Brundrit, G. B., & Taunton-Clark, J. (1986). On the existence of an El Niño-type phenomenon in the Benguela system. *Journal of Marine Research*, *44*(3), 495-520. doi: 10.1357/002224086788403105
42. Schwing, F. B., Murphree, T., & Green, P. M. (2002). The evolution of oceanic and atmospheric anomalies in the northeast Pacific during the El Niño and La Niña events of 1995–2001. *Progress in Oceanography*, *54*(1), 459-491. doi: 10.1016/S0079-6611(02)00064-2
43. Sydeman, W. J., García-Reyes, M., Schoeman, D. S., Rykaczewski, R. R., Thompson, S. A., Black, B. A., & Bograd, S. J. (2014). Climate change and wind intensification in coastal upwelling ecosystems. *Science*, *345*(6192), 77-80. doi: 10.1126/science.1251635
44. Thompson, S. A., Sydeman, W. J., Santora, J. A., Black, B. A., Suryan, R. M., Calambokidis, J., ... & Bograd, S. J. (2012). Linking predators to seasonality of upwelling: using food web indicators and path analysis to infer trophic connections. *Progress in Oceanography*, *101*(1), 106-120. doi: 10.1016/j.pocean.2012.02.001
45. Tim, N., Zorita, E., & Hünicke, B. (2015). Decadal variability and trends of the Benguela upwelling system as simulated in a high-resolution ocean simulation. *Ocean Science*, 11(3), 483. doi: 10.5194/os-11-483-2015
46. Wang, D., Gouhier, T. C., Menge, B. A., & Ganguly, A. R. (2015). Intensification and spatial homogenization of coastal upwelling under climate change. *Nature*, *518*(7539), 390-394. doi: 10.1038/nature14235
47. Wells, B. K., Field, J. C., Thayer, J. A., Grimes, C. B., Bograd, S. J., Sydeman, W. J., ... & Hewitt, R. (2008). Untangling the relationships among climate, prey and top predators in an ocean ecosystem. *Marine Ecology Progress Series*, *364*, 15-29. doi: 10.3354/meps07486
48. Zebiak, S. E. (1993) Air–sea interaction in the equatorial Atlantic region. *Journal of Climate, 6*(8), 1567-1586.

Supplemental Material

A comparison of modes of upwelling variability in the Benguela and California current ecosystems

Marisol García-Reyes*, Tarron Lamont, William J. Sydeman, Bryan A. Black, Ryan R. Rykaczewski, Sarah Ann Thompson, Steven J. Bograd.

* Corresponding author e-mail: marisolgr@faralloninstitute.org

The northern border of the Benguela Current System is located, on average, around 17°S (*Hutching et al., 2009*), the location of the Angola Front. Due to the data set grid cell distribution, the northern points are located at 14.75°S and 17.25°S. In this analysis we chose to include the cell grid that spans to 14.75°S to capture the full variability of the northern boundary of the Benguela system. A comparison between the regional averages of monthly CUI for the Northern Benguela region including (spans to 14.75°S) and excluding the northern most grid cell (17.25°S) showed only minimal differences between the magnitude and variability of the CUI (Figure SM1). The difference between both regional averages is, on average, about 1% of the CUI magnitude, and their regional monthly anomalies (as well as the monthly data) are tightly correlated ($\rho = 0.99$, $p < 0.0001$, Figure SM2). Given the similarities between these time series with different regional ranges, we chose to use the one that spans to 14.75°S since it covers times when the Angola Front is located north of its average location, therefore consistently including the entire BCS northern areas.

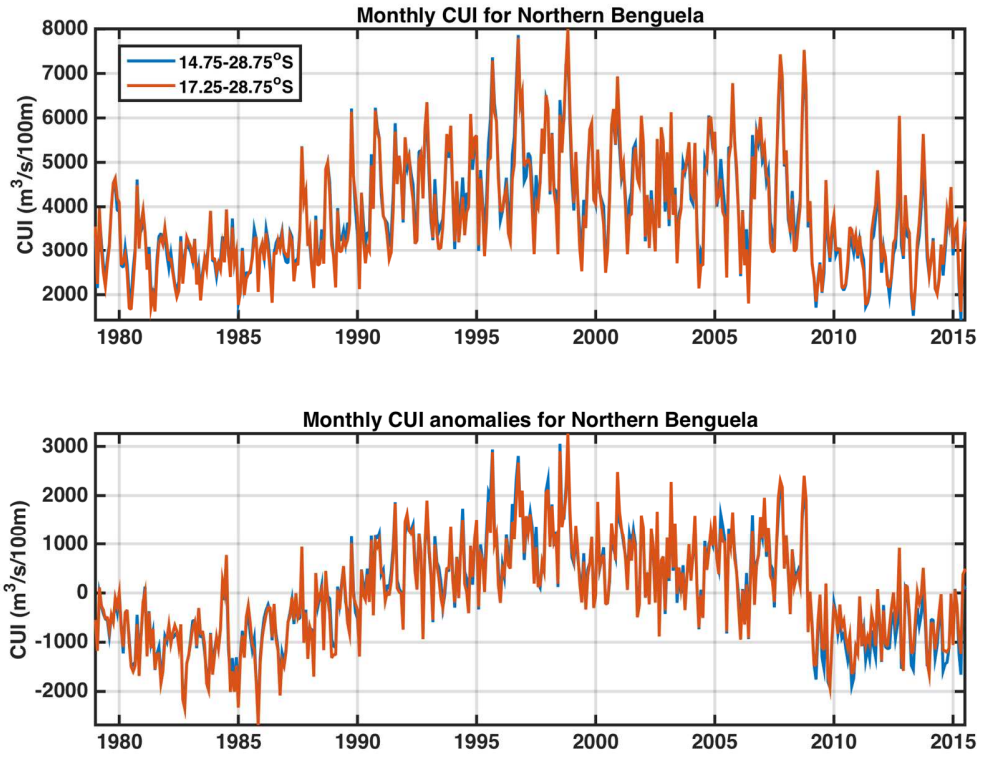

Figure SM1. Time series of monthly CUI (top) and monthly CUI anomalies (bottom) for the Northern Benguela region including the grid cell centered in 16°S (blue), and excluding that grid cell (red).

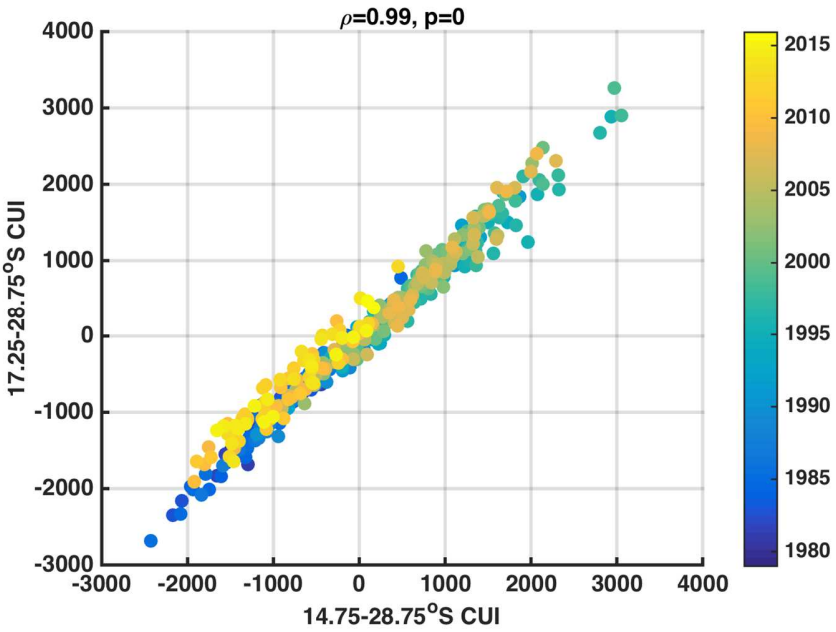

Figure SM2. Scatterplot of monthly CUI anomalies for the Northern Benguela region including the grid cell centered in 16°S (x-axis) and excluding that grid cell (y-axis). Ranked correlation coefficient and significance are shown at the top ($p<0.0001$). Colors indicate the date. CUI anomalies units are $m^3/s/100$ m.

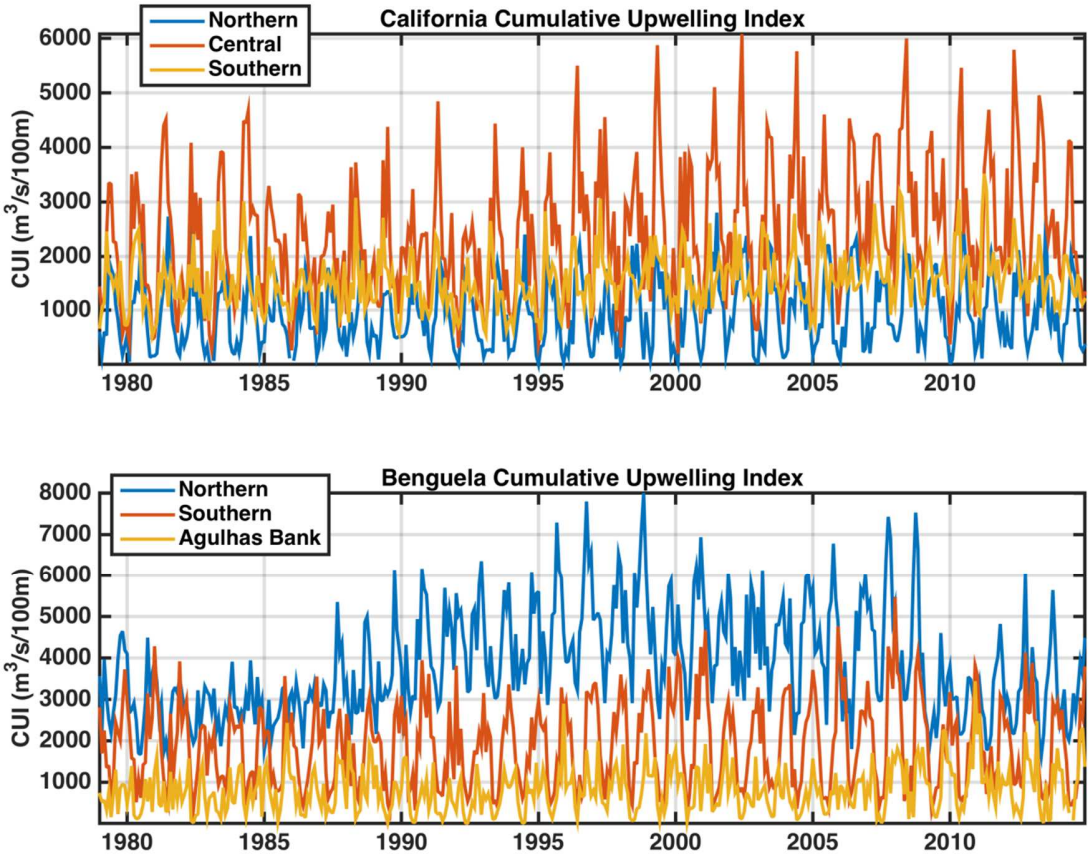

Figure SM3. Time series of monthly CUI for all regions.

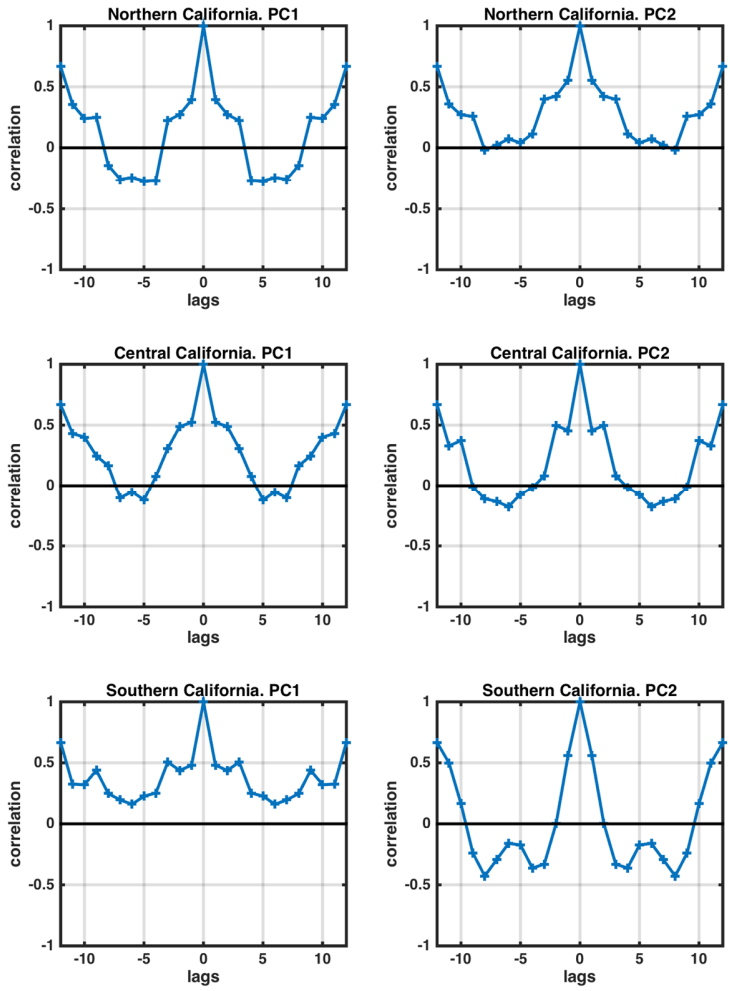

Figure SM4. Autocorrelation plots of modes coefficients for California.

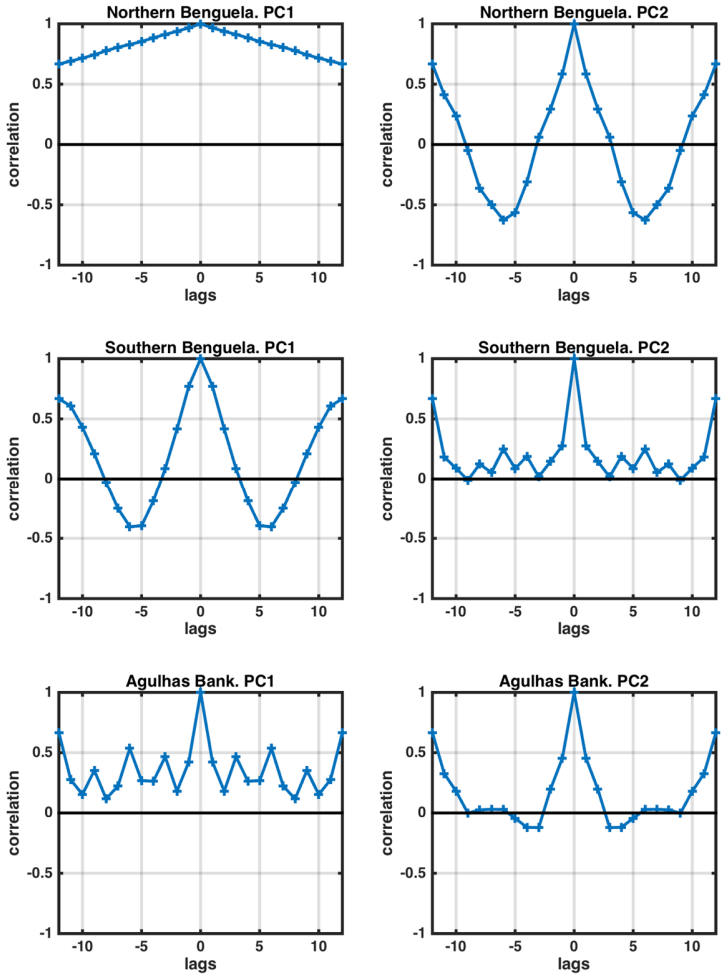

Figure SM5. Autocorrelation plots of modes coefficients for Benguela.

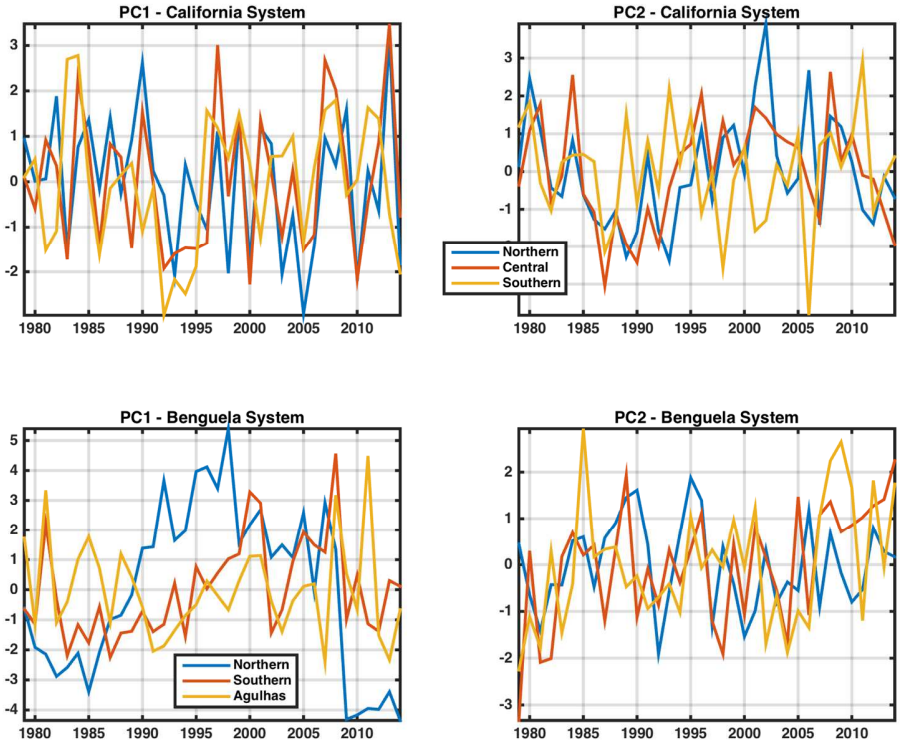

Figure SM6. Scores (time series) of PC for all regions in both systems.

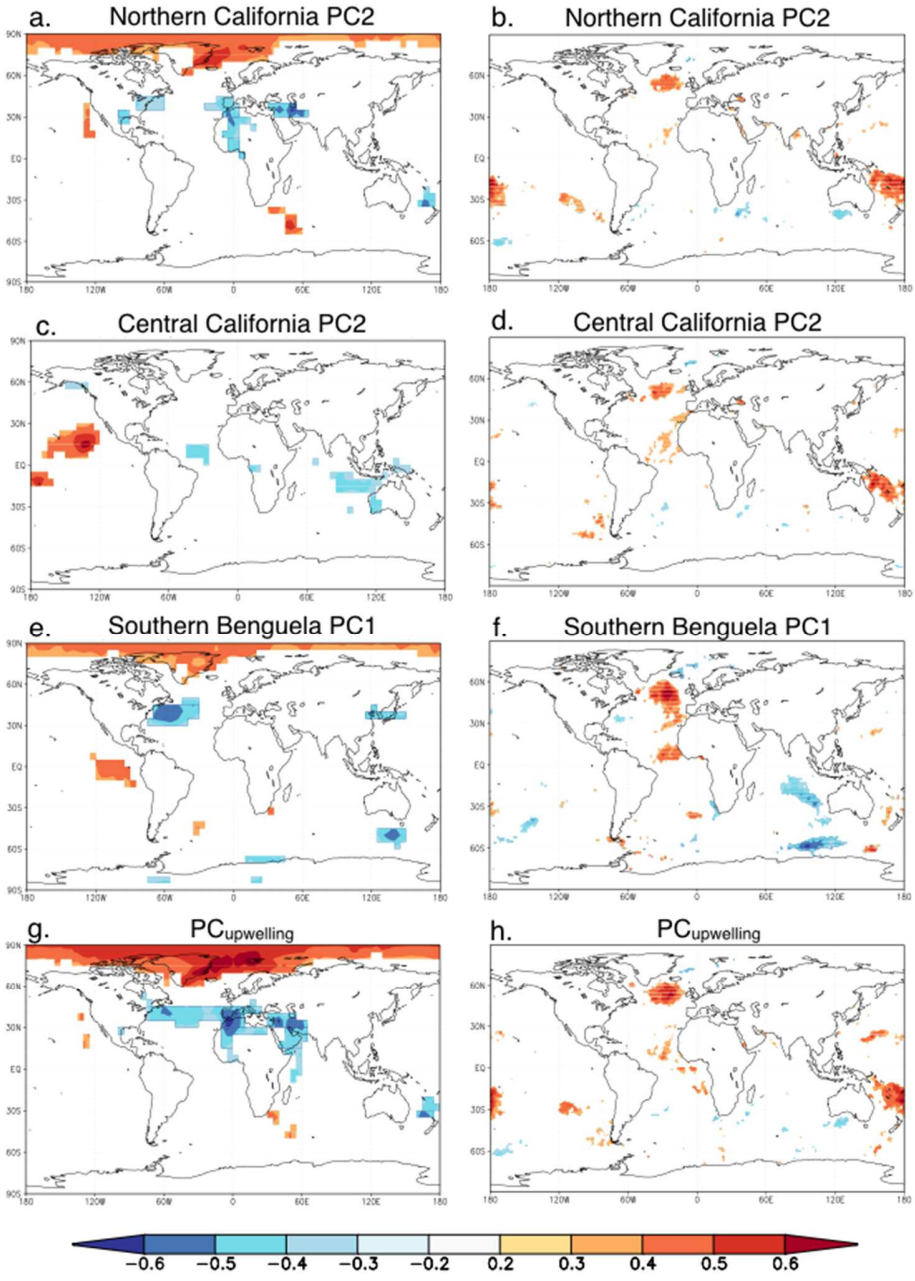

Figure SM7. Rank correlations between seasonal upwelling modes of variability and 3-month average sea level pressure (HadSLP2), and SST fields (HadISST1) ($p < 0.05$ shown) for the period 1979-2014. Northern California PC2 and (a) Feb.-Apr. SLP, (b) Feb.-Apr. SST; central California PC2 with (c) Mar-May. SLP and (d) Feb.-Apr. SST; southern Benguela PC1 with (e) Mar.-May SLP and (f) Mar.-May SST; $PC_{upwelling}$ with (g) Mar.-May SLP and (h) Mar.-May SST.

59

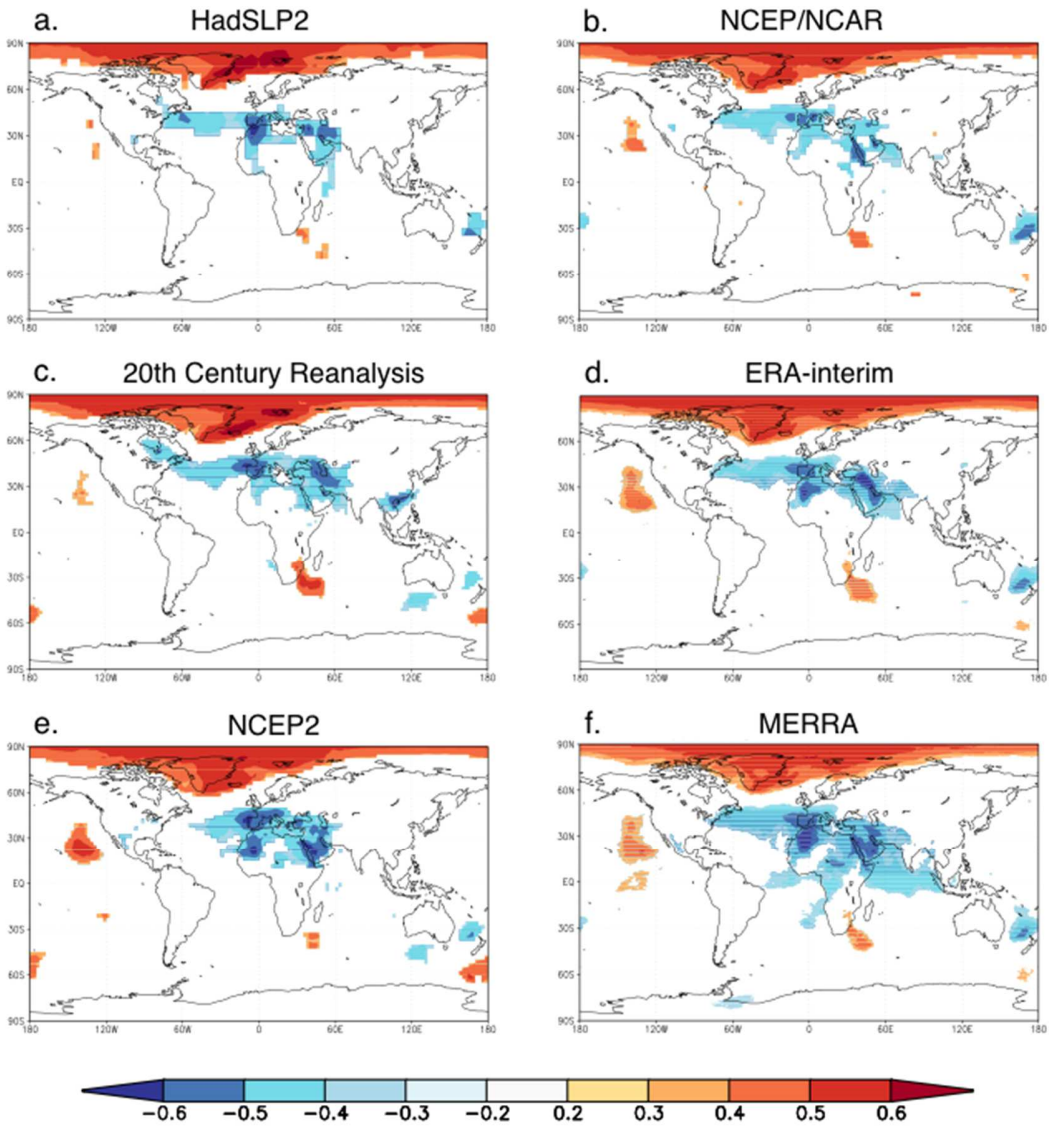

60

61 Figure SM8. Rank correlations between $PC_{upwelling}$ and March-May average sea level
62 pressure fields ($p < 0.05$ shown) for datasets: a) HadSLP2 (1979-2014), b)
63 NCEP/NCAR (1979-2014), c) 20th Century Reanalysis (1979-2011), d) ERA-interim
64 (1979-2010), e) NCEP2 (1979-2014), and f) MERRA (1980-2014).